



# Impacts of Arctic warming on ice nucleating particles over recent decades: Distributions and contributions of dust, marine organic aerosols, and bioaerosols

Zhaoyi Ren<sup>1</sup>, Kei Kawai<sup>1</sup>, Mingxu Liu<sup>1,2</sup>, and Hitoshi Matsui<sup>1</sup>

5 <sup>1</sup>Graduate School of Environmental Studies, Nagoya University, Nagoya, Japan.

<sup>2</sup>State Key Laboratory of Regional Environment and Sustainability, College of Environmental Sciences and Engineering, Peking University, Beijing, China.

**Correspondence:** Hitoshi Matsui (matsui@nagoya-u.jp)

**Abstract.** Aerosols serve as ice nucleating particles (INPs) and play a critical role in the formation of mixed-phase clouds. These clouds are prevalent in the lower and middle troposphere of the Arctic and exert a strong influence on both regional and global climate. However, limited understanding of INP sources and their temperature-dependent behavior has hindered accurate predictions of aerosol-cloud interactions in the Arctic. In this study, we investigate the sources, spatial distributions, seasonal variations, and long-term changes of INPs in the Arctic using a global climate-aerosol model that explicitly represents INPs from three Arctic aerosol species: mineral dust, marine organic aerosols (MOA), and bioaerosols. Simulations covering the period 1981–2020 show that Arctic-sourced INPs account for more than 70% of total INPs in the Arctic lower troposphere. Dust is the largest contributor (36%), followed by bioaerosols (28%) and MOA (9%). They exhibit distinct spatial and seasonal patterns, underscoring the importance of representing multiple INP species and applying appropriate parameterizations for each when modeling INPs and mixed-phase clouds in the Arctic. Over the past four decades, Arctic warming increases local emissions of all three aerosol species by 4.7–18% because of the retreat of snow and sea ice. Nevertheless, INP concentrations in the Arctic lower troposphere decline by 19–29%, primarily because the INPs per unit aerosol mass decrease with increasing temperature. This indicates that the temperature-driven reduction of ice nucleating efficiency outweighs the emission-driven increase of INP abundance, except in regions with substantial local increases of emissions.

## 1 Introduction

Mixed-phase clouds, which consist of supercooled liquid droplets and ice crystals, are widespread in the middle and lower troposphere of the Arctic and play a critical role in the Arctic climate system (Korolev et al., 2017). These clouds typically form at temperatures between  $-38\text{ }^{\circ}\text{C}$  and  $0\text{ }^{\circ}\text{C}$ , where ice formation requires the presence of aerosol particles that serve as ice nucleating particles (INPs)—a process known as heterogeneous ice nucleation (Kanji et al., 2017). Among the various nucleation pathways, immersion freezing—where an INP immersed in a supercooled droplet induces freezing—is considered the primary mechanism of ice formation in such clouds (Kulkarni et al., 2020). Once ice nucleation is initiated by INPs, water vapor evaporates from surrounding liquid droplets and deposits onto growing ice crystals. Through this process, clouds shift from being dominated by many small liquid droplets to containing fewer but larger ice crystals (Lamb and Verlinde, 2011). As a result, aerosols acting as INPs can modify cloud properties such as the liquid and ice water paths, optical depth, radiative properties (Sun and Shine, 1994), lifetime, and precipitation (Carslaw, 2022). These changes may ultimately exert a substantial impact on the Arctic climate system. However, ice nucleation mediated by INPs remains one of the most inadequately understood processes in Arctic aerosol-cloud modeling. This inadequate understanding arises from the complex interactions among aerosols, atmospheric dynamics, and cloud microphysics, as well as from limited knowledge regarding the sources and



distributions of INPs.

Recent studies have indicated that glacially sourced dust emitted from exposed soil surfaces is a potentially important source of INPs in the Arctic (Tobo et al., 2019). Marine organic aerosols (MOA) released with sea spray also contribute to INP populations in remote marine regions, including the Arctic (Wilson et al., 2015). In addition, bioaerosols—particularly bacteria originating primarily from plants—are recognized as a major source of INPs that are active at relatively high temperatures ( $\geq -15$  °C) (Kawana et al., 2024; Pereira Freitas et al., 2023; Šantl-Temkiv et al., 2019). Dust, MOA, and bioaerosols are therefore considered key sources of INPs in the Arctic. These aerosol species differ in their ice nucleation active site densities either per unit mass ( $n_m$ ) or per unit surface area ( $n_s$ ), hereafter referred to as ice nucleating ability (INA) (Demott et al., 2015; Diehl and Mitra, 2015; Hummel et al., 2018; Tobo et al., 2019; Wilson et al., 2015). For example, dust emitted in the Arctic (Arctic dust) has been shown to exhibit higher INA than other mineral dust types (Tobo et al., 2019), whereas bacterial INPs maintain high INA at higher subzero temperatures (Diehl and Mitra, 2015).

The Arctic region is warming 2–4 times faster than the global average (Holland and Bitz, 2003; Rantanen et al., 2022). One key effect of Arctic warming is a reduction of aerosol INA at ambient temperature that leads to a decrease of INP concentrations in clouds ( $INP_{cloud}$ ), even if the abundance of INP-active aerosols remains unchanged. The possible increase of cloud reflectivity and cloud cover caused by this reduction of  $INP_{cloud}$  may induce negative shortwave and positive longwave cloud radiative effects (the temperature effect in Matsui et al. (2024)). Conversely, the acceleration of the retreat of sea ice and snow cover caused by Arctic warming will expose larger oceanic and terrestrial areas and enhance natural aerosol emissions (Confer and Jaeglé, 2022). This enhancement of emissions can cause an increase of  $INP_{cloud}$  that could reduce cloud reflectivity and coverage and lead to cloud radiative effects that would be opposite to those associated with declining INA (the emission effect in Matsui et al. (2024)). These counterbalancing responses of  $INP_{cloud}$  to Arctic warming—INA-driven decreases versus emission-driven increases—form complex feedbacks that modulate Arctic cloud-climate interactions (Matsui et al., 2024). Matsui et al. (2024) have shown that the increase of Arctic dust emissions by 20% over the past 40 years because of Arctic warming has substantially offset the decrease of  $INP_{cloud}$  caused by declining INA. However, that work did not consider MOA or bioaerosols. To our knowledge, no study has assessed the long-term changes of INPs due to MOA and bioaerosols while accounting for the effects of Arctic warming on both their emissions and INA. Furthermore, the spatial distributions and temporal variations of Arctic INPs from dust, MOA, and bioaerosols remain poorly understood.

Here we use a global climate-aerosol model that explicitly represents the three major INP sources—dust, MOA, and bioaerosols—as well as their INAs (Kawai et al., submitted) to evaluate the spatial distribution and seasonal variation of  $INP_{cloud}$  from these sources in the Arctic and to quantify their contributions to total  $INP_{cloud}$ . Importantly, we investigate long-term changes of  $INP_{cloud}$  in the Arctic driven by both increasing aerosol emissions and decreasing INA.

## 2 Methods

### 2.1 Global climate-aerosol model CAM-ATRAS

We used the Community Atmosphere Model (CAM) version 5 (Lamarque et al., 2012) coupled with the Aerosol Two-dimensional bin module for foRmation and Aging Simulation (CAM-ATRAS) (Matsui, 2017; Matsui and Mahowald, 2017) and the Community Land Model (CLM) version 4 (Oleson et al., 2010) within the Community Earth System Model (CESM) version 1.2.0 (Hurrell et al., 2013). CAM-ATRAS simulates 11 aerosol species, including dust, MOA, and bioaerosols (pollen, bacteria, and fungal spores), and these three are important contributors to INPs. The model explicitly represents a wide range of aerosol processes and their roles in ice nucleation. The extensive evaluation of the model in our previous studies using a variety of aerosol observations has demonstrated its reliable performance in simulating aerosol mass and number



concentrations, size distributions, and optical properties (e.g., Kawai et al., 2021a, b, 2023; Liu et al., 2024a, b; Liu and Matsui, 2022; Matsui et al., 2018a, b, 2024; Matsui and Mahowald, 2017).

In this study, “Arctic aerosols” refer specifically to dust, MOA, and bioaerosols emitted from regions north of 60 °N, while “non-Arctic aerosols” are those emitted from regions south of 60 °N. Arctic aerosols thus represent locally emitted aerosols within the Arctic, whereas non-Arctic aerosols in the Arctic are transported over long distances from mid- and low-latitudes. The model uses separate tracers for Arctic and non-Arctic aerosols, and it simulates their emission, transport, deposition, and ice nucleation processes independently. The INPs originating from Arctic aerosols are termed Arctic INPs, and those from non-Arctic aerosols are referred to as non-Arctic INPs. Total INPs are defined to be the sum of both Arctic and non-Arctic INPs.

## 2.2 Aerosol emissions and INP parameterizations

In our model, the emissions of dust, MOA, bioaerosols, and sea salt are simulated online every 30 minutes based on simulated meteorological and surface conditions (Kawai et al., submitted). Dust emission is calculated in CLM4 using an updated version of the Dust Entrainment and Deposition model (Kok et al., 2014a, b; Zender et al., 2003). The size distribution of emitted dust particles is adopted from the work of Kok (2011). The emission of bioaerosols is calculated following the approach of Hoose et al. (2010), with separate emission fluxes calculated for pollen, bacteria, and fungal spores. The total bioaerosol emission is the sum of the emissions from these three components. Because both dust and bioaerosols are emitted from land surfaces not covered by snow and ice, their emissions are strongly influenced by the fraction of terrestrial snow and ice cover. The model incorporates an MOA emission calculation scheme derived from Burrows et al. (2013), in which the amount of MOA emissions depends on sea salt emissions (Mårtensson et al., 2003; Monahan et al., 1983). Since MOA and sea salt are emitted only from ice-free oceans, these aerosol emissions in the Arctic are closely linked to the fraction of seawater covered by ice. For aerosol emissions due to anthropogenic and biomass burning, the model uses the Coupled Model Intercomparison Project Phase 6 (CMIP6) emission dataset (Hoesly et al., 2018; van Marle et al., 2017).

This study focuses on INPs in immersion/condensation freezing processes and uses a model improved by Kawai et al. (submitted).  $INP_{cloud}$  is calculated online based on simulated ambient temperature, aerosol concentrations, INA, and the fraction of stratus clouds. The calculation includes aerosol species such as dust, MOA, bioaerosols, and black carbon. Species-specific INP parameterizations, as outlined below, are used to account for the temperature dependence of INA based on observational data. Different parameterizations are used in the model for Arctic dust INPs and non-Arctic dust INPs because of the higher INA of Arctic dust INPs, as shown by Tobo et al. (2019). The INP concentrations are calculated following Kawai et al. (2023) for Arctic dust and DeMott et al. (2015) for non-Arctic dust. MOA INPs are computed using the parameterization of Wilson et al. (2015). Bioaerosol-derived INPs, including INPs from pollen, bacteria, and fungal spores, are treated individually. Pollen INPs are parameterized according to the approach of Diehl and Mitra (2015), while fungal spore INPs follow the parameterization of Hummel et al. (2018). The model includes two key fungal spore species: spores from *Cladosporium* sp. and *Mortierella alpina*. Bacterial INPs are calculated using two different parameterizations: one based on Diehl and Mitra (2015) (Base simulation) and the other on Hummel et al. (2018) (LowBac simulation). Compared to the parameterization of Diehl and Mitra (2015), the scheme of Hummel et al. (2018) exhibits lower bacterial INA at high subzero temperatures (> -15 °C). We mainly show the results of the Base simulation, but the results of both simulations are compared in Section 3.5.

## 2.3 Simulation setups

Model simulations were conducted for 41 years from 1980 to 2020. The first year was treated as the model spin-up, and the subsequent 40 years (from 1981 to 2020) were used for analysis. The horizontal resolution of the model is  $1.9^\circ \times 2.5^\circ$ . The model uses 30 vertical layers, spanning from the surface to ~40 km. The model timestep is 30 minutes. Because Arctic mixed-



115 phase clouds predominantly occur in the lower to middle troposphere, we focus mainly on the lower troposphere ( $> 730$  hPa)  
across the Arctic region ( $> 60$  °N) unless otherwise specified.

Temperature and horizontal wind fields in the free troposphere ( $< 800$  hPa) were nudged by the Modern-Era Retrospective  
analysis for Research and Applications version 2 (MERRA-2). Sea surface temperature and sea ice data were prescribed using  
the Hadley Centre Global Sea Ice and Sea Surface Temperature (HadISST) and the NOAA 1/4° Daily Optimum Interpolation  
120 Sea Surface Temperature (OISST) dataset (Hurrell et al., 2008).

#### 2.4 Validation by observations

To evaluate the model performance in capturing the temperature dependence of INPs in the Arctic, we carried out offline  
calculations of INP number concentrations and compared the results with INP observations in northern Norway (Conen et al.,  
2016); Alert, Canada (Mason et al., 2016); Ny-Ålesund, Svalbard (Tobo et al., 2019); and Utqiagvik, Alaska, and northern  
125 Greenland (Wex et al., 2019) in the Arctic. The locations of the observational sites are shown in Fig. S1.

We performed three distinct sets of offline calculations for INP number concentrations at temperatures ranging from  $-30$  °C  
to  $-5$  °C based on simulated aerosol concentrations at the observation sites in the Arctic. For two of these calculations (Base  
and LowBac), we used the INP parameterizations described in Section 2.2: the Base case applied the Diehl and Mitra (2015)  
parameterization for bacterial INPs, while the LowBac case adopted the Hummel et al. (2018) parameterization, which assumes  
130 lower INA for bacteria. A third calculation, NoBac, excluded bacterial INPs entirely. In each calculation, total INP number  
concentrations were computed as the sum of concentrations from all relevant aerosol species—including Arctic dust, non-  
Arctic dust, MOA, fungal spores, pollen, black carbon, and bacteria (included differently in the Base and LowBac simulations).  
For each of these three offline calculations, temperatures were selected to match the observed values, and INP number  
concentrations were averaged over the period 2010–2019 for the months corresponding to each observational dataset.

### 135 3 Results and Discussion

#### 3.1 Comparisons with INP observations

On a global scale, including MOA and bioaerosols improved the agreement between simulated and observed INPs (Kawai et  
al., submitted). Among the Arctic INP observations, the discrepancies between simulated and observed INP number  
concentrations are within an order of magnitude for all three cases (Base, LowBac, and NoBac) at Alert, Ny-Ålesund in March,  
140 and northern Greenland (Figs. 1b, 1d, and 1f). This indicates that the model captures INP concentrations well at these sites.  
However, at northern Norway and Utqiagvik at  $-15$  °C and  $-10$  °C, the Base case overestimates INP concentrations by more  
than an order of magnitude (Figs. 1a and 1e). The LowBac and NoBac cases show better agreement with the observations at  
these two sites. The overestimation of total INP concentrations in the Base case may therefore be due to an overestimation of  
bacterial INPs at relatively higher temperatures ( $> -15$  °C). At Ny-Ålesund in July, all three cases overestimate INP  
145 concentrations at temperatures of  $-25$  °C to about  $-10$  °C (Fig. 1c). This overestimation is likely due to the overestimation of  
dust emissions around Svalbard (Kawai et al., 2023). These results suggest the importance of selecting appropriate INP  
parameterizations for each aerosol species, as well as a suitable combination of INP parameterizations when simulating aerosol  
INPs in the Arctic. As described in Section 2.2, this study focuses primarily on the Base simulation in subsequent sections. In  
Section 3.5, we also consider the results of the LowBac simulation by taking into account the overestimation of INPs observed  
150 in Northern Norway and Utqiagvik.

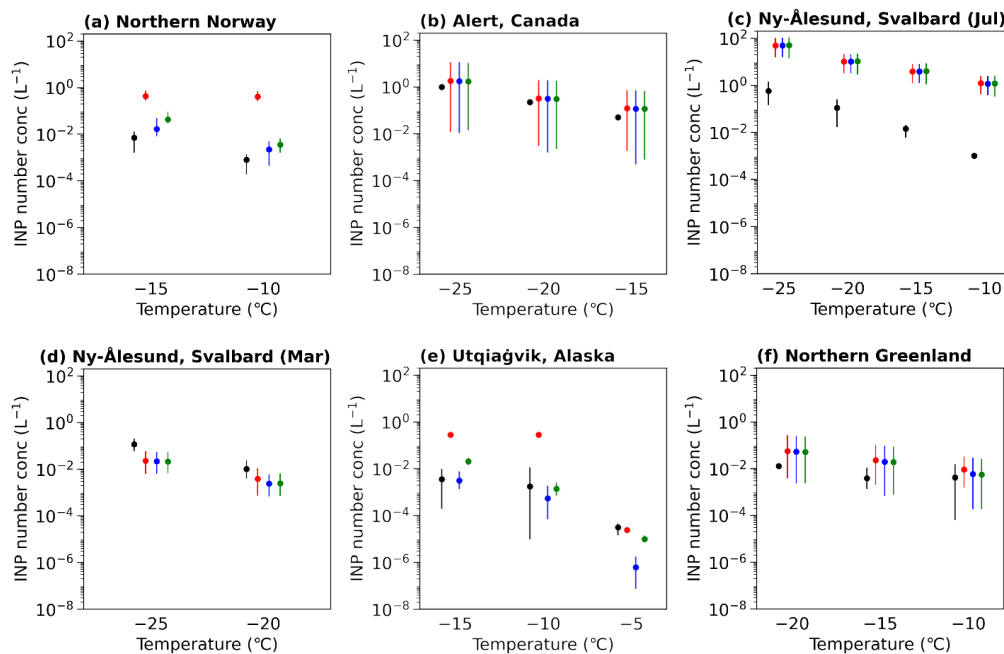


**Figure 1.** Temperature dependence of INP number concentrations at various Arctic locations: **(a)** Northern Norway, **(b)** Alert, Canada, **(c)** and **(d)** Ny-Ålesund, Svalbard (July and March, respectively), **(e)** Utqiagvik, Alaska, and **(f)** Northern Greenland. Data points represent the mean INP number concentrations, and the error bars indicate interannual variability (maximum–minimum ranges). Observational data are shown in black. Simulated total INP number concentrations from the Base simulation are shown in red, while those excluding bacterial contributions (NoBac case) are in blue. Results from the LowBac simulation are shown in green. Simulated INP number concentrations were calculated offline using parameterizations from the Base and LowBac simulations for the same months as the observations during 2010–2019.

### 160 3.2 Spatial distributions and seasonal variations of Arctic aerosols and INPs

From 1981 to 2020, the average emissions of Arctic dust, Arctic MOA, and Arctic bioaerosols are 44 Tg y<sup>-1</sup>, 0.28 Tg y<sup>-1</sup>, and 6.8 × 10<sup>22</sup> y<sup>-1</sup>, respectively. Arctic dust is emitted primarily from islands in the central Arctic Ocean (Fig. 2a). The emissions of Arctic MOA are distributed mainly along coastal regions, especially around the Greenland Sea and Norwegian Sea (Fig. 2b). Arctic bioaerosols are emitted widely from continental Arctic regions, including northern parts of Canada, Russia, and Fennoscandia (Fig. 2c). In the Arctic lower troposphere, these aerosols are distributed in regions corresponding to their respective emission sources, with vertically mean atmospheric concentrations of Arctic dust, Arctic MOA, and Arctic bioaerosols of 3.8 × 10<sup>2</sup> ng m<sup>-3</sup>, 4.3 ng m<sup>-3</sup>, and 2.8 × 10<sup>3</sup> m<sup>-3</sup>, respectively (Fig. 2d–f). Aerosols in these regions consequently act as INPs and contribute to ice crystal formation in clouds. The vertically mean INP concentrations are 0.46 m<sup>-3</sup>, 0.11 m<sup>-3</sup>, and 0.35 m<sup>-3</sup> for Arctic dust, Arctic MOA, and Arctic bioaerosols, respectively (Fig. 2g–i).



170

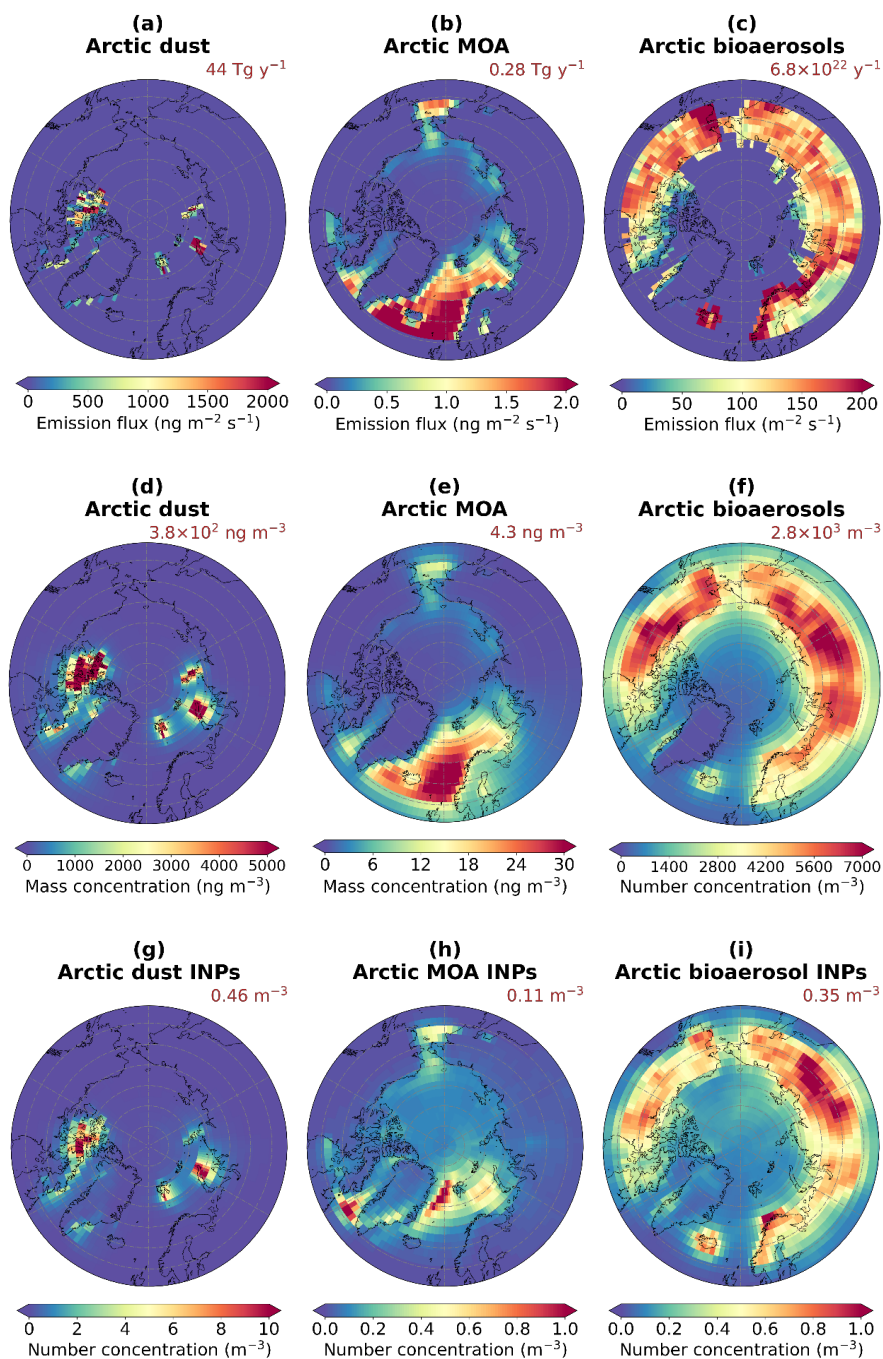


**Figure 2.** Spatial distributions of Arctic dust, Arctic MOA, and Arctic bioaerosols in the Arctic lower troposphere (> 730 hPa) averaged over 1981–2020, for (a–c) emission fluxes, (d–f) atmospheric concentrations, and (g–i) INP number concentrations. The numbers in the upper right corner of each panel represent the 40-year mean values in the Arctic lower troposphere.

In the Arctic, Arctic dust, Arctic MOA, and Arctic bioaerosols are distributed predominantly near the surface (Fig. 3a–c). Their highest concentrations occur during summer and early fall (June–September) because of the retreat of snow and sea ice



as well as enhanced growth of vegetation that results from higher summer temperatures. Notably, Arctic MOA is present year-round, and the seasonal variations of Arctic MOA concentrations are weaker than those of Arctic dust and Arctic bioaerosols.

180

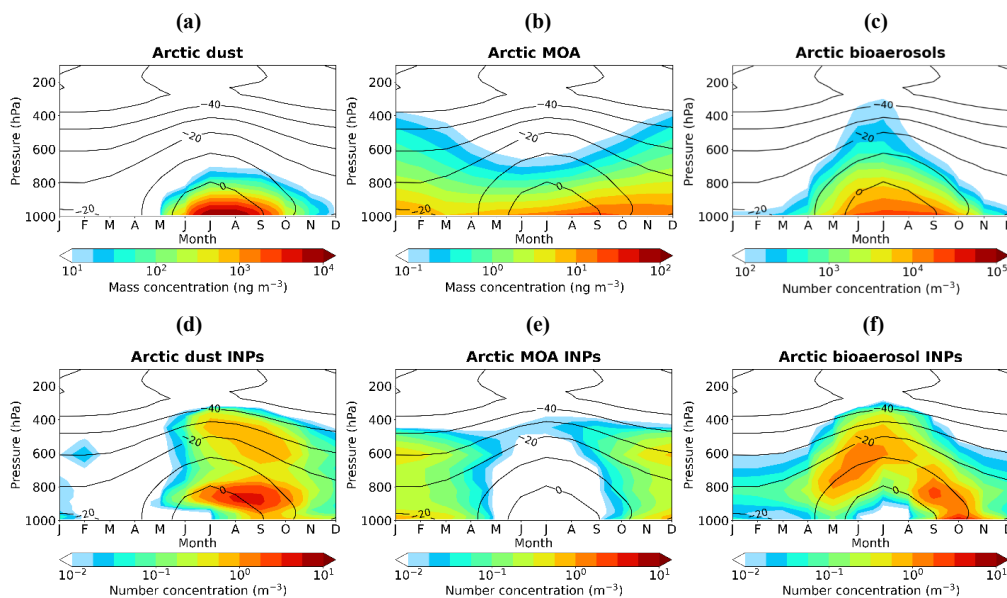


**Figure 3.** Vertical distributions and temporal variations of Arctic dust, Arctic MOA, and Arctic bioaerosols for (a–c) atmospheric concentrations and (d–f) INP number concentrations. Data are averaged over the Arctic region during 1981–2020. Black lines indicate monthly mean Arctic temperatures.

Arctic aerosol INPs exhibit broader vertical distributions and are more prevalent during colder seasons than Arctic aerosol concentrations because INAs increase exponentially with decreasing temperature (Fig. 3d–f). Concentrations of Arctic dust INPs are high in both summer and fall, not only near the surface but also at altitudes of 400–700 hPa, where temperatures are lower (around  $-30\text{ }^{\circ}\text{C}$  to  $-20\text{ }^{\circ}\text{C}$ ). Concentrations of Arctic MOA INPs are high during spring, fall, and winter, and they are highest in the middle and lower troposphere during winter. In summer, Arctic MOA INPs are present in the middle troposphere at a temperature of about  $-30\text{ }^{\circ}\text{C}$ . Arctic bioaerosol INPs are present in the Arctic throughout the year, and their simulated concentrations are highest in the middle troposphere during summer and in the lower troposphere during fall. The high number concentrations of Arctic bioaerosol INPs in warmer regions ( $> -15\text{ }^{\circ}\text{C}$ ) are attributable to the high INA of bacteria at temperatures above  $-15\text{ }^{\circ}\text{C}$  (Diehl and Mitra, 2015).

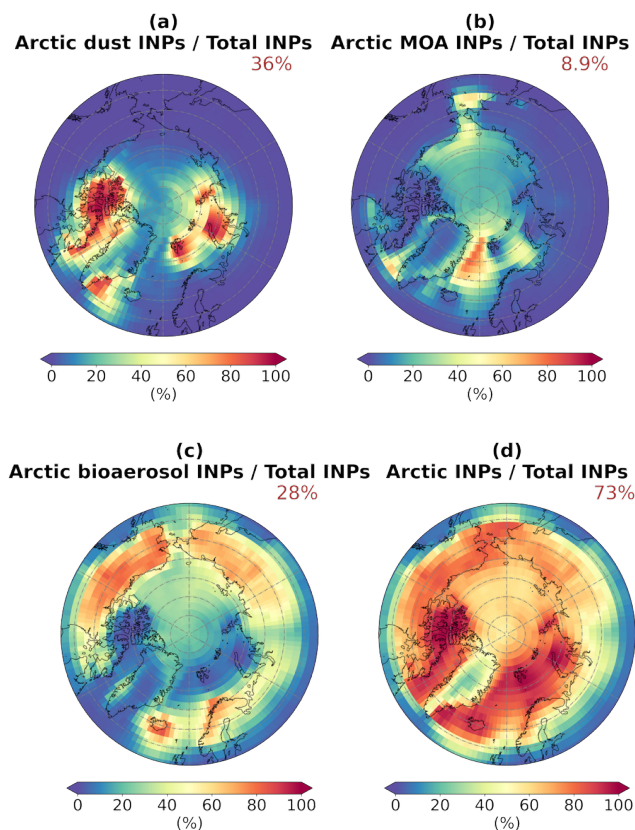
These results indicate that the spatiotemporal variations of Arctic INPs are primarily controlled by both aerosol emissions and INA in the Arctic. The distinct spatial distributions and seasonal variations of the three species of INPs highlight the importance of explicitly representing Arctic dust, Arctic MOA, Arctic bioaerosols, and their associated INPs in models because they are not yet comprehensively treated in most aerosol models.

### 200 3.3 Contribution of Arctic INPs to total INPs

In the Arctic lower troposphere, Arctic INPs (i.e., INPs from aerosols emitted in the Arctic) contribute more than 70% of the total INPs (the sum of Arctic and non-Arctic INPs) over the 40-year period (Fig. 4). Arctic dust, Arctic MOA, and Arctic bioaerosols account for 36%, 8.9%, and 28%, respectively, of the total INPs over the same period. In the lower troposphere, Arctic dust is the primary contributor to the total (Arctic + non-Arctic) INPs over islands in the central Arctic Ocean (Fig. 4a).

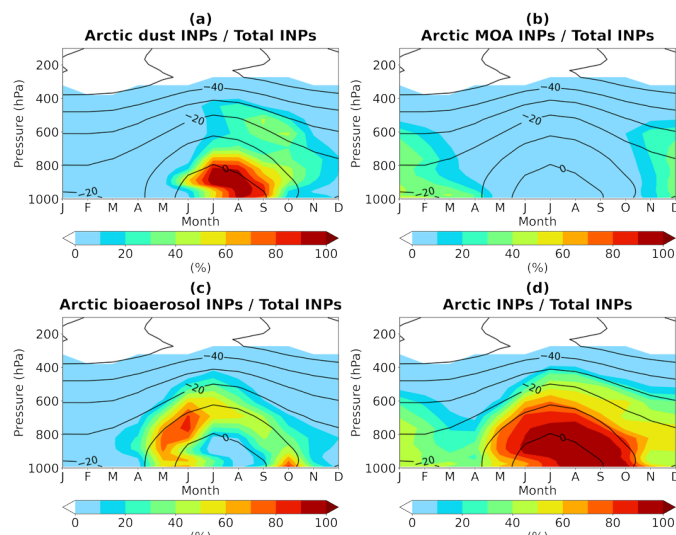


205 Arctic MOA INPs dominate over the Arctic Ocean, especially near coastal areas (Fig. 4b), while Arctic bioaerosol INPs are predominant over Arctic continental regions (Fig. 4c). As a result, Arctic INPs dominate total INPs in most regions of the Arctic lower troposphere over the four decades (Fig. 4d).



210 **Figure 4.** Spatial distributions of the contributions of (a) Arctic dust, (b) Arctic MOA, (c) Arctic bioaerosols, and (d) Arctic INPs to total (Arctic + non-Arctic) INPs in the Arctic lower troposphere (> 730 hPa) during 1981–2020. The numbers in the upper right corner of each panel are the mean contributions in the Arctic lower troposphere over the 40 years.

Arctic dust INPs dominate in summer; Arctic MOA INPs contribute 20–30% of total INPs in spring and winter; and Arctic bioaerosol INPs play a significant role from spring to fall over regions with temperatures around  $-10\text{ }^{\circ}\text{C}$  (Fig. 5). Arctic INPs contribute primarily to total INP concentrations in the lower troposphere from summer to fall, whereas total INPs in the upper troposphere at around  $-40\text{ }^{\circ}\text{C}$  to  $-30\text{ }^{\circ}\text{C}$  are mainly controlled throughout the year by aerosols transported from middle and low latitudes (Fig. 5d). The contribution of Arctic INPs to total INPs is less than 10% in the middle and upper troposphere (Fig. 5d).



220

**Figure 5.** Vertical and temporal variations of the contributions of (a) Arctic dust, (b) Arctic MOAs, (c) Arctic bioaerosols, and (d) Arctic INPs to total INPs in the Arctic during 1981–2020. Black lines indicate monthly mean Arctic temperatures.

### 3.4 Changes in Arctic aerosols and INPs over the past four decades

The annual mean surface air temperature in the Arctic increases by 1.6 °C, from –9.5 °C during 1981–1990 to –7.8 °C during 2011–2020 (Fig. S2). Snow and sea ice cover in the Arctic decrease from 68% to 66% and from 59% to 52%, respectively, during the same time interval. This warming trend extends across the Arctic, with snow and sea ice melting over nearly all land and ocean regions (Fig. 6). The largest increases of surface air temperatures occur on islands and coastal areas in the central Arctic Ocean. Major snowmelt is observed on islands in the central Arctic Ocean, including Svalbard and the Queen Elizabeth Islands, as well as in northern Europe around Scandinavia. The sea ice retreat is most severe in the coastal regions of the Arctic Ocean. These results illustrate the strong correlation between rising Arctic surface air temperature and decreasing snow and sea ice cover.

230

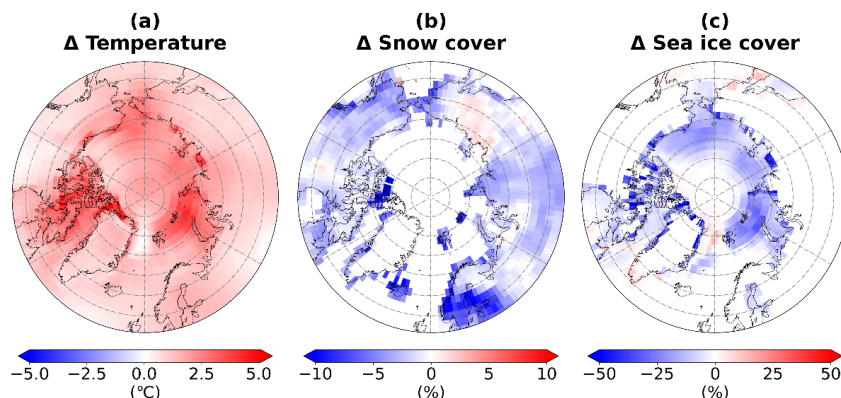


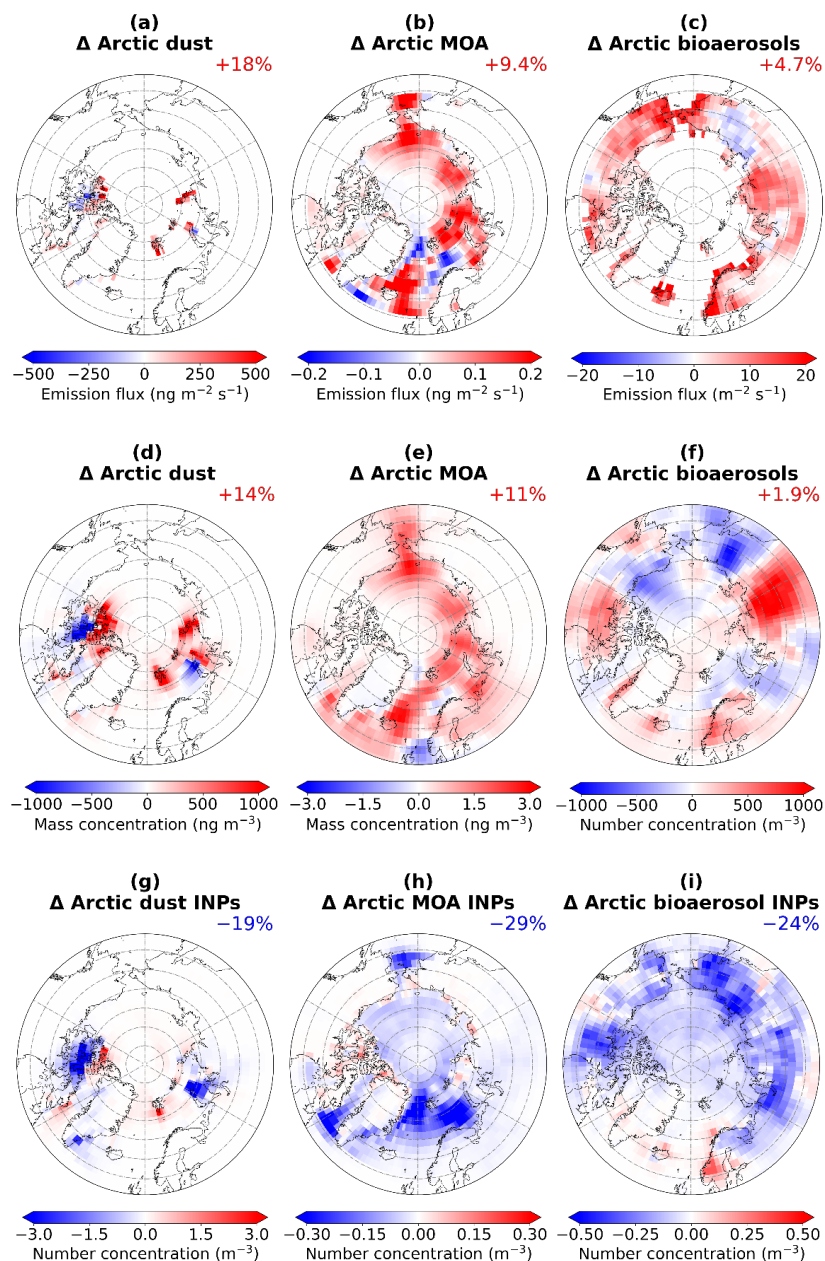
**Figure 6.** Spatial distributions of changes in (a) surface temperature, (b) snow cover, and (c) sea ice cover in the Arctic from 1981–1990 to 2011–2020.

235

As a result of the decrease of snow and ice cover, the emissions of Arctic dust, Arctic MOA, and Arctic bioaerosols increase



by 18% (from  $39 \text{ Tg y}^{-1}$  to  $46 \text{ Tg y}^{-1}$ ), 9.4% (from  $0.27 \text{ Tg y}^{-1}$  to  $0.29 \text{ Tg y}^{-1}$ ), and 4.7% (from  $6.7 \times 10^{22} \text{ y}^{-1}$  to  $7.0 \times 10^{22} \text{ y}^{-1}$ ), respectively, from 1981–1990 to 2011–2020 (Figs. 7a–c and S3a–c), though interannual variability is large (Fig. S4a–c). The vertically mean atmospheric concentrations in the Arctic lower troposphere ( $> 730 \text{ hPa}$ ) also increase. Specifically, the mean mass concentrations of Arctic dust and Arctic MOA increase by 14% (from  $3.5 \times 10^2 \text{ ng m}^{-3}$  to  $4.0 \times 10^2 \text{ ng m}^{-3}$ ) and 11% (from  $4.1 \text{ ng m}^{-3}$  to  $4.5 \text{ ng m}^{-3}$ ), respectively (Figs. 7d–e and S3d–e). The mean number concentration of Arctic bioaerosols increases by 1.9% (from  $2.8 \times 10^3 \text{ m}^{-3}$  to  $2.9 \times 10^3 \text{ m}^{-3}$ ) (Figs. 7f and S3f).



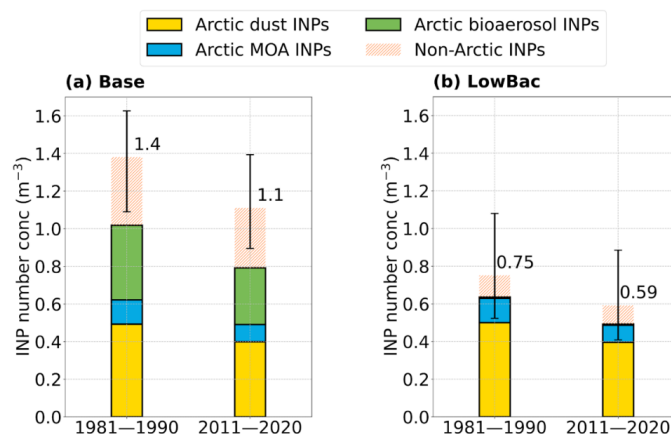


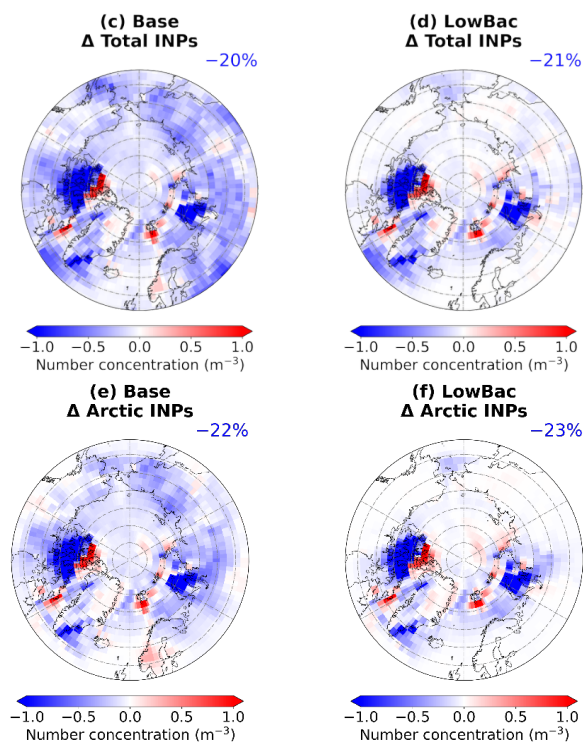
245 **Figure 7.** Spatial distributions of changes in Arctic dust, Arctic MOA, and Arctic bioaerosols for (a–c) emission fluxes, (d–f) atmospheric concentrations, and (g–i) INP number concentrations in the Arctic lower troposphere (> 730 hPa) from 1981–1990 to 2011–2020. The numbers in the upper right corner of each panel represent the rates of change in the mean Arctic lower tropospheric values between 1981–1990 and 2011–2020.

Figure 7a–c shows the spatial correlations between the increase of aerosol emissions and the reduction of snow and sea ice. For example, the increase of Arctic dust emissions is primarily concentrated over islands in the central Arctic Ocean, including Svalbard and the Queen Elizabeth Islands, where snow cover declines significantly. Likewise, the increase of Arctic MOA emissions is pronounced along coastal regions surrounding the Arctic Ocean, where there is substantial sea ice loss. Arctic bioaerosol emissions increase extensively over Arctic continental regions, particularly across Scandinavia, where there is a decline of snow cover. Conversely, Arctic bioaerosol emissions decrease over eastern Russia, where snow cover increases slightly over the four decades. These results indicate that the retreat of terrestrial snow and sea ice between 1981–1990 and 2011–2020, driven by Arctic warming, led to increased emissions and atmospheric concentrations of Arctic dust, Arctic MOA, and Arctic bioaerosols.

While Arctic aerosol emissions increase over the four decades, concentrations of Arctic INPs decline (Fig. S4g–i). In the Arctic lower troposphere, the mean INP number concentrations from Arctic dust, Arctic MOA, and Arctic bioaerosols decrease by 19% (from 0.49 m<sup>-3</sup> to 0.40 m<sup>-3</sup>), 29% (from 0.13 m<sup>-3</sup> to 0.09 m<sup>-3</sup>), and 24% (from 0.40 m<sup>-3</sup> to 0.30 m<sup>-3</sup>), respectively (Figs. 7g–i and S3g–i). The number concentrations of Arctic dust INPs decline across islands in the central Arctic Ocean, except for areas with notable increases of Arctic dust emissions, such as Svalbard and the Queen Elizabeth Islands. Arctic MOA INPs decrease over the Arctic Ocean during the past four decades. Arctic bioaerosol INPs decrease across most regions, particularly over the continents, except over Scandinavia, where Arctic bioaerosol emissions increase substantially.

265 The number concentrations of Arctic INPs and total INPs in the Arctic lower troposphere decrease by 22% and 20%, respectively, from 1981–1990 to 2011–2020 (Fig. 8a). The decrease of total INPs in the Arctic lower troposphere is broadly simulated over islands in the central Arctic Ocean, coastal waters, and continents (Fig. 8c). However, total INPs increase over some regions where there is a strong growth of aerosol emissions. The spatial distribution of the changes of Arctic INPs is similar to that of total INPs (Fig. 8e). These results indicate that changes of the total INP number concentrations in the Arctic lower troposphere over the past 40 years are driven largely by a reduction of INPs originating from the Arctic.





**Figure 8.** Decadal changes of INP number concentrations in the Arctic lower troposphere (> 730 hPa) between 1981–1990 and 2011–2020. 275 **(a–b)** Mean INP number concentrations in the Arctic lower troposphere during 1981–1990 and 2011–2020 for the **(a)** Base and **(b)** Lowbac simulations. **(c–f)** Spatial distributions of changes in INP number concentrations between 1981–1990 and 2011–2020. Panels **(c–d)** show total INP concentrations for the **(c)** Base and **(d)** LowBac simulations, while panels **(e–f)** show Arctic INP (Arctic dust INPs + Arctic MOA INPs + Arctic bioaerosol INPs) concentrations for the **(e)** Base and **(f)** LowBac simulations. In panels **(a)** and **(b)**, Arctic dust, Arctic MOA, Arctic bioaerosols, and non-Arctic aerosols (i.e., aerosols emitted from south of 60 °N) are shown in yellow, blue, green, and orange, 280 respectively. Error bars represent interannual variability (maximum–minimum ranges) for each period. In panels **(c–f)**, the numbers in the upper right corner indicate the rates of change of mean values in the Arctic lower tropospheric between 1981–1990 and 2011–2020.

INP number concentrations of Arctic aerosols decrease over the last four decades, regardless of the increase of Arctic aerosol emissions. Changes of Arctic INPs are controlled by the balance between the increase of INPs caused by increasing emissions (emission effect) and the decrease of INPs caused by decreasing INA (temperature effect) (Matsui et al., 2024). The 285 results of this study indicate that the temperature effect outweighs the emission effect in the Arctic for all INP species considered in this study (dust, MOAs, and bioaerosols emitted in the Arctic), at least from 1981 to 2020. In other words, INA changes associated with Arctic warming are the dominant factor controlling changes of Arctic INPs associated with climate change in the Arctic during that time. The results of this study also indicate that the emission effect can be more important than the temperature effect in regions where Arctic aerosol emissions increase substantially. These results suggest that a better 290 understanding of aerosol emissions and INA and their changes in the Arctic is required for more accurate estimates of INPs and their effects on clouds in the Arctic.

### 3.5 Sensitivity of INPs to bacterial INA

As noted in Section 3.1, the Base case overestimates bacterial INP number concentrations in Northern Norway and Utqiagvik. This study therefore also considers an alternative parameterization for calculating bacterial INPs (Hummel et al., 2018) that is



295 used in the LowBac simulation. This section presents the results of the LowBac simulation and compares them with those of  
the Base simulation.

The number concentration of Arctic bioaerosol INPs in the Arctic lower troposphere in the LowBac simulation is less  
than 2% of that in the Base simulation (Fig. S3i). The LowBac simulation produces much lower bioaerosol INPs throughout  
the lower Arctic atmosphere, but the characteristics of their spatial distribution are similar to those in the Base simulation  
300 during 1981–2020 (Fig. S5).

In the LowBac simulation, the simulated Arctic bioaerosol INPs are highest at high altitudes during summer at around  
−30 °C in the Arctic (Fig. S6). The high bacterial INP concentrations at relatively high subzero temperatures (around −10 °C)  
seen in the Base simulation are not evident in the LowBac simulation. Similarly, the LowBac simulation produces lower Arctic  
INP concentrations than the Base simulation at around −10 °C.

305 The contribution of Arctic INPs to total INPs also differs between the LowBac and Base simulations (Fig. S6). In the  
LowBac simulation, Arctic INPs contribute over 80% to total INPs in the Arctic lower troposphere during 1981–2020  
compared with a contribution of 73% in the Base simulation. Arctic dust, Arctic MOA, and Arctic bioaerosols account for 66%,  
16%, and 0.89% of the total INPs, respectively (Fig. S5b). Arctic bioaerosols make a much smaller contribution to total INPs  
over continental areas in the LowBac simulation than the Base case.

310 Despite this substantial difference, there is a decreasing trend of Arctic bioaerosol INP number concentrations during  
1981–2020 in both simulations. The decrease in the LowBac simulation is 25%, from 0.0067 m<sup>−3</sup> (1981–1990) to 0.0050 m<sup>−3</sup>  
(2011–2020) (Fig. S3i). The lower concentration of Arctic bioaerosol INPs in the LowBac simulation leads to lower  
concentrations of both Arctic INPs and total INPs (Fig. 8b). In the Arctic lower troposphere, the mean number concentrations  
of Arctic and total INPs in the LowBac simulation decline by 23% (from 0.64 m<sup>−3</sup> to 0.49 m<sup>−3</sup>) and 21% (from 0.75 m<sup>−3</sup> to  
315 0.59 m<sup>−3</sup>), respectively, from 1981–1990 to 2011–2020. While the magnitudes of the concentrations differ considerably, the  
rates of reduction over the four decades are nearly identical in the Base and LowBac simulations.

Overall, compared to the Base simulation, the LowBac simulation produces much lower Arctic bioaerosol INP  
concentrations that lead to lower concentration of Arctic INPs and total INPs. The result is better agreement with the  
observations in Northern Norway and Alaska, although both simulations perform well at the other three observation sites.  
320 Recent studies have shown a strong correlation between atmospheric concentration of INPs and bacterial marker genes in the  
Arctic summer (Kawana et al., 2024; Šantl-Temkiv et al., 2019). Pereira Freitas et al. (2023) have indicated that most of the  
high-temperature INPs are driven by biological sources, suggesting that bioaerosols are a significant source of INPs in the  
Arctic. This implication contrasts with the low concentration and contribution of bioaerosol INPs in the LowBac simulation.  
In addition, our recent study has shown that the Base simulation generally reproduced observed INPs and their temperature  
325 dependence on a global scale (Kawai et al., submitted). These results highlight the significant uncertainties in current bacterial  
INP parameterizations; different parameterizations can drastically change the simulated bioaerosol INPs and their importance.  
Further studies are therefore necessary to obtain a deeper understanding of bioaerosol INA.

#### 4 Conclusions

In this study, we simulated inter-annual changes of aerosols and ice nucleation in mixed-phase clouds in the Arctic during  
330 1981–2020 with three primary INP species—dust, MOA, and bioaerosols—that were incorporated into a global climate-  
aerosol model. The reasonable agreement between our model simulations and INP observations at Alert, Ny-Ålesund in March,  
and northern Greenland show the reliability of the model in simulating INPs. However, the model overestimates INPs at high  
subzero temperatures (> −15 °C) in Northern Norway, Utqiagvik, and Ny-Ålesund in July, likely due to the overestimation of



bacterial INPs in Northern Norway and Utqiagvik and of dust emissions around Svalbard at Ny-Ålesund in July.

335 Our simulations show that Arctic INPs dominate total INPs in the Arctic lower troposphere, with Arctic dust (36%) being the largest contributor, followed by Arctic bioaerosols (28%) and Arctic MOA (8.9%). In contrast, INPs in the middle and upper troposphere are derived primarily from aerosols transported from non-Arctic sources. The three Arctic INP species exhibit distinct spatial patterns that closely correspond to those of their aerosol sources. Arctic dust INPs dominate over islands in the central Arctic Ocean. Arctic MOA INPs are most prominent in coastal regions of the Arctic Ocean. Arctic bioaerosol INPs primarily affect land areas. In addition, this study reveals clear differences in the vertical distributions and seasonal variations of Arctic INPs among the three species. Arctic dust INPs are abundant in summer at higher altitudes (400–700 hPa), where temperatures range from  $-30\text{ }^{\circ}\text{C}$  to  $-20\text{ }^{\circ}\text{C}$ . Arctic MOA INPs peak during spring and winter in the middle troposphere near  $-30\text{ }^{\circ}\text{C}$ . Concentrations of Arctic bioaerosol INPs are elevated during summer and early fall at temperatures around  $-10\text{ }^{\circ}\text{C}$ . These results highlight the importance of simultaneously considering multiple aerosol species that serve as INPs when

340 INPs primarily affect land areas. In addition, this study reveals clear differences in the vertical distributions and seasonal variations of Arctic INPs among the three species. Arctic dust INPs are abundant in summer at higher altitudes (400–700 hPa), where temperatures range from  $-30\text{ }^{\circ}\text{C}$  to  $-20\text{ }^{\circ}\text{C}$ . Arctic MOA INPs peak during spring and winter in the middle troposphere near  $-30\text{ }^{\circ}\text{C}$ . Concentrations of Arctic bioaerosol INPs are elevated during summer and early fall at temperatures around  $-10\text{ }^{\circ}\text{C}$ . These results highlight the importance of simultaneously considering multiple aerosol species that serve as INPs when

345 predicting their spatial distributions and temporal variations in the Arctic.

Aerosol emissions increased by 18%, 9.4%, and 4.7% for Arctic dust, Arctic MOA, and Arctic bioaerosols, respectively, from 1981–1990 to 2011–2020, mainly because of the melting of snow and sea ice (Fig. 9). In contrast, Arctic INP concentrations decreased by 19%, 29%, and 24% as a result of the reduced INA associated with Arctic warming. This contrast suggests that changes of INA (i.e., the temperature effect) have a greater influence on INP concentrations than increasing

350 emissions (i.e., the emission effect), except in regions where emissions increase substantially and thus outweigh the temperature effect. These findings highlight the strong influence of warming on Arctic INP concentrations, through its effects on both aerosol emissions and INA.

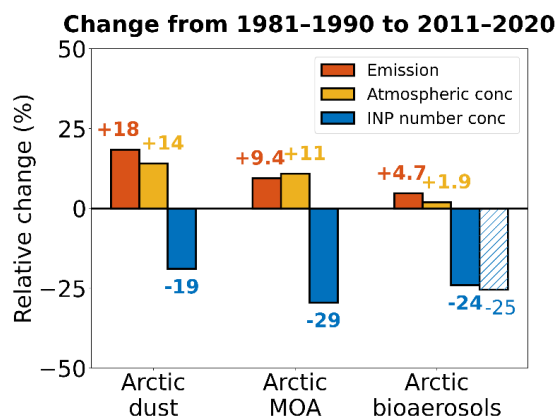


**Figure 9.** Changes of Arctic dust, Arctic MOA, and Arctic bioaerosols and their associated INPs from 1981–1990 to 2011–2020. Changes in emissions (red), vertically averaged atmospheric concentrations (yellow), and vertically averaged INP number concentrations (blue) are shown for the Arctic lower troposphere ( $> 730\text{ hPa}$ ) from the Base simulation. The hatched bar indicates the result from the LowBac simulation. The numbers above each bar indicate the rates of change in the mean values in the Arctic lower troposphere between 1981–1990 and 2011–2020.

355

A comparison of the two parameterizations for bacterial INA (Base and LowBac) underscores the significant impact of choices of INP parameterization on the simulation results. While the Base simulation produces bioaerosol INP concentrations approximately 50 times those in the LowBac simulation, the spatial distributions and the rates of reduction from 1981–1990 to 2011–2020 are generally consistent between the two simulations.

360

Overall, this study highlights the critical importance of selecting appropriate INP parameterizations for each aerosol species



in order to accurately simulate INPs and mixed-phase clouds in the Arctic lower troposphere. Reducing uncertainties in the  
365 INP parameterizations of bioaerosols is particularly crucial given the good agreement between observations and the Base  
simulation on a global scale as well as the recent observational studies that have emphasized the significance of bioaerosols  
for Arctic INPs. A better understanding of the interplay between aerosol emissions, INA, the contributions of these two factors  
to Arctic cloud dynamics, and their temporal variations under Arctic warming is essential for improving predictions of Arctic  
climate change and its broader impacts on the global climate system. These findings contribute to advancing our understanding  
370 of the complex feedback mechanisms in the Arctic and provide a foundation for future research on INP-related processes in  
polar climates.

#### **Author contributions**

ZR and HM conceived and designed the study and interpreted the results. KK contributed to model improvement. ZR and ML  
performed the model simulations and data analysis. ZR drafted the manuscript. All authors discussed the results and contributed  
375 to the manuscript.

#### **Acknowledgement**

This work was partly achieved through the use of the SQUID supercomputer at the D3 Center, Osaka University.

#### **Financial support**

This research was supported by the Ministry of Education, Culture, Sports, Science, and Technology (MEXT) and the Japan  
380 Society for the Promotion of Science (JSPS) through KAKENHI Grants (JP22H03722, JP23H00515, JP23H00523,  
JP23K18519, JP23K24976, and JP24H02225); the MEXT Arctic Challenge for Sustainability II (ArCS II;  
JPMXD1420318865) and 3 (ArCS-3; JPMXD1720251001) projects; the Environment Research and Technology Development  
Fund 2-2301 (JPMEERF20232001) of the Environmental Restoration and Conservation Agency; and the National Institute of  
Polar Research (NIPR) through Special Collaboration Project no. B25-02. Z.R. was supported by the THERS Make New  
385 Standards Program for the Next Generation Researchers at Nagoya University.

#### **Data availability**

Data used in this study are available upon request from the corresponding authors (HM).

#### **Code availability**

The codes used to conduct the analysis presented in this paper are available from the corresponding author upon reasonable  
390 request.

#### **Competing interests**

The authors declare no conflict of interests.



## References

- Burrows, S. M., Hoose, C., Pöschl, U., and Lawrence, M. G.: Ice nuclei in marine air: biogenic particles or dust?, *Atmos Chem Phys*, 13, 245–267, <https://doi.org/10.5194/acp-13-245-2013>, 2013.
- Carlslaw, K. S.: *Aerosols and Climate*, <https://doi.org/10.1016/C2019-0-00121-5>, 2022.
- Conen, F., Stopelli, E., and Zimmermann, L.: Clues that decaying leaves enrich Arctic air with ice nucleating particles, *Atmos Environ*, 129, 91–94, <https://doi.org/10.1016/j.atmosenv.2016.01.027>, 2016.
- Confer, K. and Jaeglé, L.: Impact of Changing Arctic Sea Ice Extent, Sea Ice Age, and Snow Depth on Sea Salt Aerosol from Blowing Snow and the Open Ocean for 1980-2017, United States -- Washington, 41 pp., 2022.
- Demott, P. J., Prenni, A. J., McMeeking, G. R., Sullivan, R. C., Petters, M. D., Tobo, Y., Niemand, M., Möhler, O., Snider, J. R., Wang, Z., and Kreidenweis, S. M.: Integrating laboratory and field data to quantify the immersion freezing ice nucleation activity of mineral dust particles, *Atmos Chem Phys*, 15, <https://doi.org/10.5194/acp-15-393-2015>, 2015.
- Diehl, K. and Mitra, S. K.: New particle-dependent parameterizations of heterogeneous freezing processes: sensitivity studies of convective clouds with an air parcel model, *Atmos Chem Phys*, 15, 12741–12763, <https://doi.org/10.5194/acp-15-12741-2015>, 2015.
- Hoesly, R. M., Smith, S. J., Feng, L., Klimont, Z., Janssens-Maenhout, G., Pitkanen, T., Seibert, J. J., Vu, L., Andres, R. J., Bolt, R. M., Bond, T. C., Dawidowski, L., Kholod, N., Kurokawa, J., Li, M., Liu, L., Lu, Z., Moura, M. C. P., O'Rourke, P. R., and Zhang, Q.: Historical (1750–2014) anthropogenic emissions of reactive gases and aerosols from the Community Emissions Data System (CEDS), *Geosci Model Dev*, 11, 369–408, <https://doi.org/10.5194/gmd-11-369-2018>, 2018.
- Holland, M. M. and Bitz, C. M.: Polar amplification of climate change in coupled models, *Clim Dyn*, 21, 221–232, <https://doi.org/10.1007/s00382-003-0332-6>, 2003.
- Hoose, C., Kristjánsson, J. E., and Burrows, S. M.: How important is biological ice nucleation in clouds on a global scale?, *Environmental Research Letters*, 5, 024009, <https://doi.org/10.1088/1748-9326/5/2/024009>, 2010.
- Hummel, M., Hoose, C., Pummer, B., Schaupp, C., Fröhlich-Nowoisky, J., and Möhler, O.: Simulating the influence of primary biological aerosol particles on clouds by heterogeneous ice nucleation, *Atmos Chem Phys*, 18, <https://doi.org/10.5194/acp-18-15437-2018>, 2018.
- Hurrell, J. W., Hack, J. J., Shea, D., Caron, J. M., and Rosinski, J.: A new sea surface temperature and sea ice boundary dataset for the community atmosphere model, *J Clim*, 21, <https://doi.org/10.1175/2008JCLI2292.1>, 2008.
- Hurrell, J. W., Holland, M. M., Gent, P. R., Ghan, S., Kay, J. E., Kushner, P. J., Lamarque, J.-F., Large, W. G., Lawrence, D., Lindsay, K., Lipscomb, W. H., Long, M. C., Mahowald, N., Marsh, D. R., Neale, R. B., Rasch, P., Vavrus, S., Vertenstein, M., Bader, D., Collins, W. D., Hack, J. J., Kiehl, J., and Marshall, S.: The Community Earth System Model: A Framework for Collaborative Research, *Bull Am Meteorol Soc*, 94, 1339–1360, <https://doi.org/10.1175/BAMS-D-12-00121.1>, 2013.
- Kanji, Z. A., Ladino, L. A., Wex, H., Boose, Y., Burkert-Kohn, M., Cziczo, D. J., and Krämer, M.: Overview of Ice Nucleating Particles, *Meteorological Monographs*, 58, 1.1-1.33, <https://doi.org/10.1175/AMSMONOGRAPHS-D-16-0006.1>, 2017.
- Kawai, K., Matsui, H., and Tobo, Y.: High potential of Asian dust to act as ice nucleating particles in mixed-phase clouds simulated with a global aerosol-climate model, *Journal of Geophysical Research: Atmospheres*, 126, <https://doi.org/10.1029/2020JD034263>, 2021a.
- Kawai, K., Matsui, H., Kimura, R., and Shinoda, M.: High sensitivity of Asian dust emission, transport, and climate impacts to threshold friction velocity, *Scientific Online Letters on the Atmosphere*, 17, <https://doi.org/10.2151/SOLA.2021-042>, 2021b.



- Kawai, K., Matsui, H., and Tobo, Y.: Dominant role of Arctic dust with high ice nucleating ability in the Arctic lower troposphere, *Geophys Res Lett*, 50, <https://doi.org/10.1029/2022GL102470>, 2023.
- 435 Kawai, K., Ren, Z., and Matsui, H.: Global Modeling of Ice Nucleating Particles of Multiple Aerosol Species and Associated Cloud Radiative Effects, *EGUsphere* [preprint], <https://doi.org/10.5194/egusphere-2025-5850>, 2026.
- Kawana, K., Taketani, F., Matsumoto, K., Tobo, Y., Iwamoto, Y., Miyakawa, T., Ito, A., and Kanaya, Y.: Roles of marine biota in the formation of atmospheric bioaerosols, cloud condensation nuclei, and ice-nucleating particles over the North Pacific Ocean, Bering Sea, and Arctic Ocean, *Atmos Chem Phys*, 24, <https://doi.org/10.5194/acp-24-1777-2024>, 2024.
- 440 Kok, J. F.: A scaling theory for the size distribution of emitted dust aerosols suggests climate models underestimate the size of the global dust cycle, *Proceedings of the National Academy of Sciences*, 108, 1016–1021, <https://doi.org/10.1073/pnas.1014798108>, 2011.
- Kok, J. F., Mahowald, N. M., Fratini, G., Gillies, J. A., Ishizuka, M., Leys, J. F., Mikami, M., Park, M.-S., Park, S.-U., Van Pelt, R. S., and Zobeck, T. M.: An improved dust emission model – Part 1: Model description and comparison against  
445 measurements, *Atmos Chem Phys*, 14, 13023–13041, <https://doi.org/10.5194/acp-14-13023-2014>, 2014a.
- Kok, J. F., Albani, S., Mahowald, N. M., and Ward, D. S.: An improved dust emission model – Part 2: Evaluation in the Community Earth System Model, with implications for the use of dust source functions, *Atmos Chem Phys*, 14, 13043–13061, <https://doi.org/10.5194/acp-14-13043-2014>, 2014b.
- Korolev, A., McFarquhar, G., Field, P. R., Franklin, C., Lawson, P., Wang, Z., Williams, E., Abel, S. J., Axisa, D., Borrmann, S., Crosier, J., Fugal, J., Krämer, M., Lohmann, U., Schlenzcek, O., Schnaiter, M., and Wendisch, M.: Mixed-Phase Clouds: Progress and Challenges, *Meteorological Monographs*, 58, 5.1-5.50, <https://doi.org/10.1175/AMSMONOGRAPHS-D-17-0001.1>, 2017.
- Kulkarni, G., Hiranuma, N., Möhler, O., Höhler, K., China, S., Cziczo, D. J., and DeMott, P. J.: A new method for operating a continuous-flow diffusion chamber to investigate immersion freezing: assessment and performance study, *Atmos Meas  
455 Tech*, 13, 6631–6643, <https://doi.org/10.5194/amt-13-6631-2020>, 2020.
- Lamarque, J.-F., Emmons, L. K., Hess, P. G., Kinnison, D. E., Tilmes, S., Vitt, F., Heald, C. L., Holland, E. A., Lauritzen, P. H., Neu, J., Orlando, J. J., Rasch, P. J., and Tyndall, G. K.: CAM-chem: description and evaluation of interactive atmospheric chemistry in the Community Earth System Model, *Geosci Model Dev*, 5, 369–411, <https://doi.org/10.5194/gmd-5-369-2012>, 2012.
- 460 Lamb, D. and Verlinde, J.: *Physics and Chemistry of Clouds*, Cambridge University Press, <https://doi.org/10.1017/CBO9780511976377>, 2011.
- Liu, M. and Matsui, H.: Secondary Organic Aerosol Formation Regulates Cloud Condensation Nuclei in the Global Remote Troposphere, *Geophys Res Lett*, 49, <https://doi.org/10.1029/2022GL100543>, 2022.
- Liu, M., Song, Y., Matsui, H., Shang, F., Kang, L., Cai, X., Zhang, H., and Zhu, T.: Enhanced atmospheric oxidation toward  
465 carbon neutrality reduces methane’s climate forcing, *Nat Commun*, 15, 3148, <https://doi.org/10.1038/s41467-024-47436-9>, 2024a.
- Liu, M., Matsui, H., Hamilton, D. S., Rathod, S. D., Lamb, K. D., and Mahowald, N. M.: Representation of iron aerosol size distributions of anthropogenic emissions is critical in evaluating atmospheric soluble iron input to the ocean, *Atmos Chem Phys*, 24, 13115–13127, <https://doi.org/10.5194/acp-24-13115-2024>, 2024b.
- 470 van Marle, M. J. E., Kloster, S., Magi, B. I., Marlon, J. R., Daniau, A.-L., Field, R. D., Arneeth, A., Forrest, M., Hantson, S., Kehrwald, N. M., Knorr, W., Lasslop, G., Li, F., Mangeon, S., Yue, C., Kaiser, J. W., and van der Werf, G. R.: Historic global biomass burning emissions for CMIP6 (BB4CMIP) based on merging satellite observations with proxies and fire models (1750–2015), *Geosci Model Dev*, 10, 3329–3357, <https://doi.org/10.5194/gmd-10-3329-2017>, 2017.



- Mårtensson, E. M., Nilsson, E. D., de Leeuw, G., Cohen, L. H., and Hansson, H. C.: Laboratory simulations and  
475 parameterization of the primary marine aerosol production, *Journal of Geophysical Research: Atmospheres*, 108,  
<https://doi.org/10.1029/2002jd002263>, 2003.
- Mason, R. H., Si, M., Chou, C., Irish, V. E., Dickie, R., Elizondo, P., Wong, R., Brintnell, M., Elsasser, M., Lassar, W. M.,  
Pierce, K. M., Leaitch, W. R., MacDonald, A. M., Platt, A., Toom-Sauntry, D., Sarda-Estève, R., Schiller, C. L., Suski, K.  
J., Hill, T. C. J., Abbatt, J. P. D., Huffman, J. A., DeMott, P. J., and Bertram, A. K.: Size-resolved measurements of ice-  
480 nucleating particles at six locations in North America and one in Europe, *Atmos Chem Phys*, 16, 1637–1651,  
<https://doi.org/10.5194/acp-16-1637-2016>, 2016.
- Matsui, H.: Development of a global aerosol model using a two-dimensional sectional method: 1. Model design, *J Adv Model  
Earth Syst*, 9, 1921–1947, <https://doi.org/10.1002/2017MS000936>, 2017.
- Matsui, H. and Mahowald, N.: Development of a global aerosol model using a two-dimensional sectional method: 2.  
485 Evaluation and sensitivity simulations, *J Adv Model Earth Syst*, 9, 1887–1920, <https://doi.org/10.1002/2017MS000937>,  
2017.
- Matsui, H., Mahowald, N. M., Moteki, N., Hamilton, D. S., Ohata, S., Yoshida, A., Koike, M., Scanza, R. A., and Flanner, M.  
G.: Anthropogenic combustion iron as a complex climate forcer, *Nat Commun*, 9, <https://doi.org/10.1038/s41467-018-03997-0>, 2018a.
- 490 Matsui, H., Hamilton, D. S., and Mahowald, N. M.: Black carbon radiative effects highly sensitive to emitted particle size  
when resolving mixing-state diversity, *Nat Commun*, 9, 3446, <https://doi.org/10.1038/s41467-018-05635-1>, 2018b.
- Matsui, H., Kawai, K., Tobo, Y., Iizuka, Y., and Matoba, S.: Increasing Arctic dust suppresses the reduction of ice nucleation  
in the Arctic lower troposphere by warming, *NPJ Clim Atmos Sci*, 7, 266, <https://doi.org/10.1038/s41612-024-00811-1>,  
2024.
- 495 Monahan, E. C., Spiel, D. E., and Davidson, K. L.: Model of marine aerosol generation via whitecaps and wave disruption,  
[https://doi.org/10.1007/978-94-009-4668-2\\_16](https://doi.org/10.1007/978-94-009-4668-2_16), 1983.
- Oleson, K., Lawrence, D., and Kluzek, E.: Technical Description of version 4.0 of the Community Land Model (CLM), 2010.
- Pereira Freitas, G., Adachi, K., Conen, F., Heslin-Rees, D., Krejci, R., Tobo, Y., Yttri, K. E., and Zieger, P.: Regionally sourced  
bioaerosols drive high-temperature ice nucleating particles in the Arctic, *Nat Commun*, 14, <https://doi.org/10.1038/s41467-023-41696-7>, 2023.
- 500 Rantanen, M., Karpechko, A. Yu., Lipponen, A., Nordling, K., Hyvärinen, O., Ruosteenoja, K., Vihma, T., and Laaksonen, A.:  
The Arctic has warmed nearly four times faster than the globe since 1979, *Commun Earth Environ*, 3, 168,  
<https://doi.org/10.1038/s43247-022-00498-3>, 2022.
- Šantl-Temkiv, T., Lange, R., Beddows, D., Rauter, U., Pilgaard, S., Dall’osto, M., Gunde-Cimerman, N., Massling, A., and  
505 Wex, H.: Biogenic Sources of Ice nucleating Particles at the High Arctic Site Villum Research Station, *Environ Sci Technol*,  
53, <https://doi.org/10.1021/acs.est.9b00991>, 2019.
- Sun, Z. and Shine, K. P.: Studies of the radiative properties of ice and mixed-phase clouds, *Quarterly Journal of the Royal  
Meteorological Society*, 120, 111–137, <https://doi.org/10.1002/qj.49712051508>, 1994.
- Tobo, Y., Adachi, K., DeMott, P. J., Hill, T. C. J., Hamilton, D. S., Mahowald, N. M., Nagatsuka, N., Ohata, S., Uetake, J.,  
510 Kondo, Y., and Koike, M.: Glacially sourced dust as a potentially significant source of ice nucleating particles, *Nat Geosci*,  
12, <https://doi.org/10.1038/s41561-019-0314-x>, 2019.
- Wex, H., Huang, L., Zhang, W., Hung, H., Traversi, R., Becagli, S., Sheesley, R. J., Moffett, C. E., Barrett, T. E., Bossi, R.,  
Skov, H., Hünnerbein, A., Lubitz, J., Löffler, M., Linke, O., Hartmann, M., Herenz, P., and Stratmann, F.: Annual variability  
of ice-nucleating particle concentrations at different Arctic locations, *Atmos Chem Phys*, 19, 5293–5311,



515 <https://doi.org/10.5194/acp-19-5293-2019>, 2019.

Wilson, T. W., Ladino, L. A., Alpert, P. A., Breckels, M. N., Brooks, I. M., Browse, J., Burrows, S. M., Carslaw, K. S., Huffman, J. A., Judd, C., Kilhau, W. P., Mason, R. H., McFiggans, G., Miller, L. A., Najera, J. J., Polishchuk, E., Rae, S., Schiller, C. L., Si, M., Temprado, J. V., Whale, T. F., Wong, J. P. S., Wurl, O., Yakobi-Hancock, J. D., Abbatt, J. P. D., Aller, J. Y., Bertram, A. K., Knopf, D. A., and Murray, B. J.: A marine biogenic source of atmospheric ice-nucleating particles, *Nature*, 520, <https://doi.org/10.1038/nature14986>, 2015.

Zender, C. S., Bian, H., and Newman, D.: Mineral Dust Entrainment and Deposition (DEAD) model: Description and 1990s dust climatology, *Journal of Geophysical Research: Atmospheres*, 108, <https://doi.org/10.1029/2002JD002775>, 2003.